DISTRIBUTIONS OF THE ELECTRON CONCENTRATION AND THE ELECTRICAL FIELD INTENSITY IN A DISCHARGE WITH TRANSVERSE GAS PUMPING

R. F. Yunusov

UDC 537.525

Computation formulas are obtained for the parameters of a gas discharge with a transverse gas flow.

Gas-discharge parameters in the presence of a gas flow are investigated extensively in the modern stage of electronic engineering development. One of the structural schemes is a discharge that occurs in a rectangular channel with transverse gas pumping [1-4] (Fig. 1).

The gas velocity vector in this diagram is directed parallel to the positive direction of the X axis, the electric current flow along the Y axis, and the discharge is bounded in the direction of the Z axis by dielectric walls. In the general case, the discharge parameters are inhomogeneous in all three coordinates. However, as experiments [5, 6] show, a domain exists in the interelectrode gap in which the discharge parameters along the y coordinate are homogeneous. The purpose of this paper is to find theoretically the discharge parameter distribution in the domain mentioned.

It is assumed that the condition of quasineutrality is satisfied, the charged particles are formed during direct ionization and leave the volume element because of convective and ambipolar diffusion. It is considered that this particle formation occurs only in the discharge zone (ν = const, $0 \leq x \leq a$; $\nu = 0$, $x < 0$, $x > a$).

The one-dimensional problem was solved in the mentioned formulation in [4]. In a two-dimensional formulation the equation of charged particle balance is written thus

$$\frac{v}{D_a}\frac{\partial n}{\partial x} = \frac{\partial^2 n}{\partial x^2} + \frac{\partial^2 n}{\partial z^2}, \quad x<0,\ x>a, \tag{1}$$

$$\frac{v}{D_a}\frac{\partial n}{\partial x} = \frac{\partial^2 n}{\partial x^2} + \frac{\partial^2 n}{\partial z^2} + \frac{\nu}{D_a} n, \quad 0 \leqslant x \leqslant a,$$

where $0 \leq z \leq b$. We reduce (1) to dimensionless form

$$2\,\mathrm{Pe}_d \frac{\partial \bar{n}}{\partial \bar{x}} = \frac{\partial^2 \bar{n}}{\partial \bar{x}^2} + \bar{a}^2 \frac{\partial^2 \bar{n}}{\partial \bar{z}^2}, \quad \bar{x}<0, \quad \bar{x}>1, \tag{2}$$

$$2\,\mathrm{Pe}_d \frac{\partial \bar{n}}{\partial \bar{x}} = \frac{\partial^2 \bar{n}}{\partial \bar{x}^2} + \bar{a}^2 \frac{\partial^2 \bar{n}}{\partial \bar{z}^2} + \frac{\nu a^2}{D_a}\bar{n}, \quad 0 \leqslant \bar{x} \leqslant 1,$$

where $\mathrm{Pe}_d = v a/2D_a$, $\bar{x} = x/a$, $\bar{z} = z/b$, $\bar{a} = a/b$, $\bar{n} = n/c_1$, c_1 is a constant.

The electron concentration is assumed zero on the dielectric walls and at an infinite distance from the discharge zone, while continuity conditions for $\bar{n}$ and $\partial\bar{n}/\partial\bar{x}$ should be satisfied on the boundaries of zones I and II, II and III (Fig. 1). Taking account of the above-mentioned conditions, the obtained solution of (2) is the following

$$\bar{n} = (\sin \pi\bar{z}) \exp(\beta + \mathrm{Pe}_d)\bar{x}, \quad \bar{x}<0,$$

$$\bar{n} = \left[\frac{\beta}{\gamma}\sin(\gamma\bar{x}) + \cos(\gamma\bar{x})\right](\sin \pi\bar{z}) \exp(\mathrm{Pe}_d \bar{x}), \quad 0 \leqslant \bar{x} \leqslant 1, \tag{3}$$

$$\bar{n} = (\sin \pi\bar{z}) \exp[\mathrm{Pe}_d \bar{x} + \beta(1 - \bar{x})], \quad \bar{x} > 1.$$

A. N. Tupolev Kazan Aviation Institute. Translated from Inzhenerno-Fizicheskii Zhurnal, Vol. 54, No. 1, pp. 98-103, January, 1988. Original article submitted September 9, 1986.

 0022-0841/88/5401-0076 $12.50 © 1988 Plenum Publishing Corporation

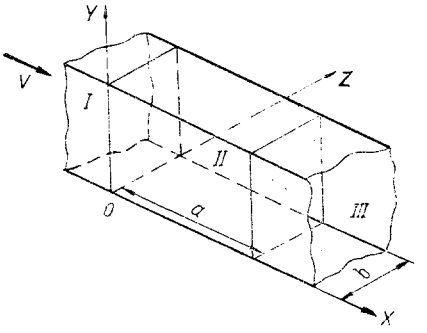

Fig. 1

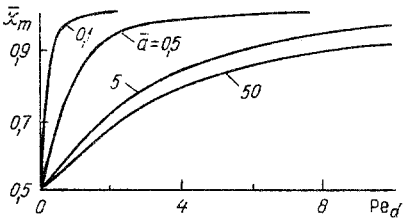

Fig. 2

Fig. 1. Discharge chamber diagram: V) gas velocity; 0) origin; I) entrance zone ($x < 0$); II) discharge zone ($0 \leq x \leq a$); III) exit zone ($x > a$).

Fig. 2. Dependence of the coordinate corresponding to the maximum electron concentration on the diffusion Péclet number.

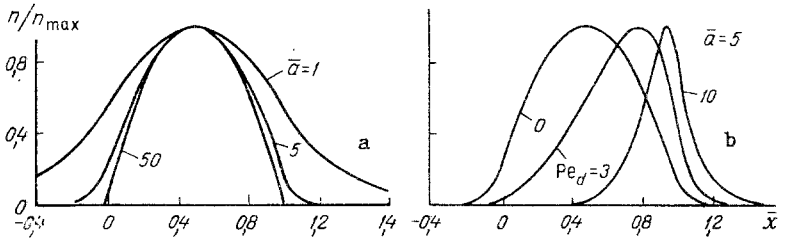

Fig. 3. Relative electron concentration distribution in the coordinate $\bar{x}$.

Here $\beta = \sqrt{Pe_d^2 + (\pi a)^2}$, $\gamma = \sqrt{\nu a^2/D_a) - \beta^2}$. A transcendental equation is also obtained here to find γ:

$$\operatorname{tg}\gamma = \frac{2\gamma\beta}{\gamma^2 - \beta^2}. \tag{4}$$

We select from the infinite set of roots of (4) those for which the condition of positivity of the electron concentration is assured in (3). These values of γ_1, dependent on $\bar{a}$ and Pe_d, are presented in Table 1. The values found for γ_1, in combination with (3), permit computation of the electron concentration distribution as well as of the ionization parameter

$$\frac{\nu a^2}{D_a} = \pi^2 \frac{a^2}{b^2} + \gamma_1^2(\bar{a}, Pe_d) + \frac{v^2 a^2}{4D_a^2}. \tag{5}$$

It follows from an analysis of (4) that the values γ_1 vary between zero and $\pi = 3.1415$. As both Pe_d increases for a given $\bar{a}$ and $\bar{a}$ for a given Pe_d, the values γ_1 grow and tend to the number π. Hence it follows that for sufficiently large values of Pe_d the first two components in the right side of (5) can be neglected in comparison with the remaining term. In this particular case an approximate formula $\nu \approx v^2/4D_a$ is obtained that is in agreement with the result in [4].

The position of the electron concentration maximum in the discharge zone is determined from the formula

$$\bar{x}_m = \frac{1}{\gamma_1} \operatorname{arctg} \frac{(\beta + Pe_d)\gamma_1}{\gamma_1^2 - \beta Pe_d}.$$

The value of $\bar{x}_m$ depends on the number Pe_d, the parameter $\bar{a}$ and varies between 0.5 and 1 (Fig. 2). Substitution of $\bar{x} = \bar{x}_m$ in (3) permits computation of n_{max}/c_1 and then the distribution of the relative electron concentration n/n_{max} in the coordinate $\bar{x}$ (Fig. 3). The electron concentration in a discharge without a gas stream (Fig. 3a) is symmetric relative to the plane $\bar{x} = \bar{x}_m = 0.5$. As the parameter $\bar{a}$ grows, the degree of inhomogeneity n/n_{max} increases in the coordinate $\bar{x}$ and, moreover the degree of charged particle localization in the

TABLE 1. Dependence of γ_1 on $\bar{a}$ and Pe_d

Pe_d	$\bar{a}$							
	0,01	0,05	0,1	0,5	1	5	10	50
0	0,250	0,553	0,773	1,571	2,005	2,790	2,954	3,102
1	1,307	1,313	1,333	1,676	2,035	2,791	2,954	3,102
5	2,284	2,285	2,286	2,311	2,376	2,805	2,956	3,102
10	2,628	2,628	2,628	2,633	2,647	2,839	2,962	3,102
20	2,858	2,858	2,858	2,859	2,861	2,913	2,982	3,102
50	3,021	3,021	3,021	3,021	3,021	3,026	3,039	3,104
100	3,080	3,080	3,080	3,080	3,080	3,081	3,083	3,108

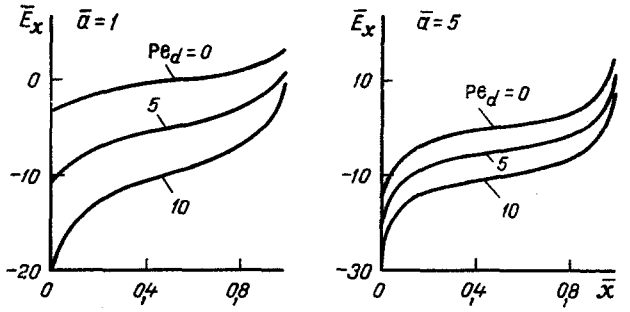

Fig. 4. Distribution of the relative electric field intensity in the coordinate $\bar{x}$.

discharge zone does also. The symmetry of the n/n_{max} distribution is spoiled in a discharge with a gas stream, and the position of the maximum electron concentration is shifted downstream.

The formula (5) can be used to determine the electron temperature by the same means as was done in [7, 8] for a discharge in a cylindrical channel without a gas stream. To use the results in [8] we represent (5) in the form

$$\frac{\nu R_{equ}^2}{D_a} = \lambda^2, \tag{6}$$

where $\lambda = 2.405$; $R_{equ} = a\lambda/\sqrt{Pe_d^2 + (\pi^2 a^2/b^2) + \gamma_1^2}$. The equivalent radius R_{equ} is the characteristic dimension of the discharge in a transverse gas stream, dependent on the geometric dimensions a and b, the number Pe_d and permitting representation of the formula (5) in the form (6), which is analogous for a discharge without a gas stream in a cylindrical channel with radius $R = R_{equ}$. An equation governing the dependence of the electron temperature on the pressure, the chamber radius R, and the species of gas was obtained in [8] for the case mentioned on the basis of the relationship (6), the formula for ν under the assumption of a Maxwell electron velocity distribution function and the expression $D_a = \mu_+ kT_e/e$. The solution of this equation was universal for all gases by a graph of the dependence of T_e/U_i on cpR, where c is a constant dependent on the species of gas [7, 9]. This same graph can be used to estimate the electron temperature in a discharge organized in a rectangular channel with a transverse gas stream if R_{equ} is substituted instead of R, after having first been computed for given geometric dimensions a and b and the number Pe_d. As the number Re_d or the parameter $\bar{a}$ increases, the equivalent radius diminishes, which indicates an increase in the electron temperature in conformity with the mentioned graph of the dependence $T_e/U_i = f(cpR)$.

The components of the electric field intensity vector in the X – Y plane in which there is no electric current are determined from the formulas $E_x = -kT_e/e\ 1/n\ \partial n/\partial x$; $E_x = -kT_e/e\ 1/n\ \partial n/\partial z$, which reduce to the following computational form after (3) has been taken into account

$$\bar{E}_x = \frac{\gamma_1 \sin(\gamma_1 \bar{x}) - \beta\cos(\gamma_1 \bar{x})}{\beta\gamma_1^{-1}\sin(\gamma_1 \bar{x}) + \cos(\gamma_1 \bar{x})} - Pe_d; \quad \bar{E}_z = -\pi \operatorname{ctg} \pi \bar{z}, \tag{7}$$

where $\bar{E}_x = E_x e a/kT_e$, $\bar{E}_z = E_z e b/kT_e$. Computations of the relative electric field intensity component in the direction of the coordinate x are represented in Fig. 4. In the absence of a gas stream the $\bar{E}_x$ distribution is symmetric relative to the middle of the discharge zone.

A gas stream causes an increase in the component $\bar{E}_x$ directed opposite to the gas velocity vector. As the number Pe_d grows, the coordinate of the point at which $\bar{E}_x$ changes sign, shifts to the right boundary of the discharge zone. The regularity mentioned was observed experimentally in [6]. For the upstream boundary of the discharge zone for the gas the first of the expressions (7) reduces to the form $(\bar{E}_x)_{x=0} = -\beta - Pe_d$. For a sufficiently large value of the number Pe_d it can approximately be considered the $(\bar{E}_x)_{x=0} \approx -2Pe_d$ or $E_x\mu_+ \approx -v$. It hence follows that the electric field component opposite to the gas stream increases approximately in proportion to the gas velocity in the mentioned discharge domain and has a magnitude such that the drift velocity of the positive ions exceeds the gas velocity, which also agrees with the data in [6].

Let us mention the sequence of computing the discharge parameters corresponding to specific experimental conditions: electrode geometry, pressure, gas species and velocity. The dimensions a and b of the discharge zone are approximately equal to the corresponding electrode dimensions. The number Pe_d is determined initially from the experimental values of a, v_{exp} and an estimate of the coefficient $(D_a)_{est}$ that is dependent on the gas pressure and the electron temperature. The $(D_a)_{theor}$ and v_{theo} are computed from the initial data a, b, p, the gas species, and Pe_d. The value of the number Pe_d is refined from a comparison of v_{theo} and v_{exp}, and the computation is repeated again. The mentioned successive approximation procedure is performed until the values v_{theo} and v_{exp} agree within the limits of gas velocity measurement error.

Let us present an example of computing the discharge parameters in a nitrogen stream under conditions corresponding to experiment [6]: a = 4 cm, b = 100 cm, p = 5.5 kPa, and v = 35 m/sec. The value Pe_d = 12 was found by the above-mentioned successive approximations method. Corresponding to this value of Pe_d and $\bar{a}$ = 0.04 are γ_1 = 2.699 and $R_{equ} \approx 0.78$ cm. From the graphs presented in [8, 9] we determine T_e = 1.15 eV and E/p = 6 V/(cm·gPa). From the first of expressions (7) we determine $(E_x/p)_{x=0}$ = 1.25 V/(cm·gPa). The coefficient $D_a \approx$ 560 cm^2/sec and the gas velocity v ≈ 33 m/sec correspond to the found value of T_e and the number Pe_d = 12. Comparison with the experiment data [6]: E/p = 9.8 V/(cm·gPa); $T_e \approx$ 1 eV: E_x/p = 5.4 V/(cm·gPa) shows satisfactory agreement with the exception of the parameter E_x/p which was obtained several times greater experimentally. The difference mentioned is explained firstly by not having taken into account a number of processes in the theoretical model, which occur under the conditions of the experiment [6], for instance, bulk recombination. Secondly, the error in the computation is associated with inaccurate assignment of the discharge zone which is selected by means of the electrode dimensions. Thirdly, only the maximal value E_x/p = 5.4 V/(cm·gPa) is presented in the spatial domain of the discharge, which cannot correspond to the computational domain.

Therefore, formulas are obtained in this paper for the computation of the distributions of the electron concentration and the electric field intensity components perpendicular to the electric current direction in a discharge with a transverse gas stream. The results emanating from the formuls are in qualitative agreement with the regularities found experimentally.

NOTATION

X, Y, Z, coordinate axes; x, y, z, Cartesian coordinates; v, gas velocity; D_a, ambipolar diffusion coefficient; ν, ionization frequency; n, electron concentration; a and b, geometric dimensions of the discharge zone; e, T_e, electron charge and temperature; μ_+, ion mobility; k, Boltzmann constant; p, gas pressure; and U_i, ionization potential.

LITERATURE CITED

1. R. I. Soloukhin (ed.), Gas Lasers [in Russian], Novosibirsk (1977).
2. E. P. Velikov, V. S. Golubev, and S. V. Pashkin, Usp. Fiz. Nauk, 137, No. 1, 117-150 (1982).
3. V. Yu. Baranov, A. A. Vedenov, and V. G. Niz'ev, Teplofiz. Vys. Temp., 10, No. 6, 1156-1159 (1972).
4. V. M. Gol'dfarb, R. I. Lyagushenko, and M. B. Tendler, Teplofiz. Vys. Temp., 13, No. 3, 497-502 (1975).
5. S. S. Vorontsov, A. I. Ivanchenko, A. A. Shepelenko, and Yu. A. Yakobi, Zh. Tekh. Fiz., 47, No. 11, 2287-2292 (1977).
6. A. I. Ivanchenko and A. A. Shepelenko, Zh. Tekh. Fiz., 51, No. 10, 2043-2092 (1981).
7. W. Schöttky, Phys. Z., 25, 342-348 (1924).

8. A. Engel, Ionized Gases [Russian translation], Moscow (1959).
9. Yu. P. Raizer, Principles of the Modern Physics of Gas Discharge Processes [in Russian], Moscow (1980).

THERMAL DESTRUCTION OF SPHERICAL ICE PARTICLES UNDER THE ACTION OF RADIATION WITH λ = 10.6 μm

A. P. Prishivalko, L. P. Semenov, L. G. Astef'eva, and S. T. Leiko

UDC 551.511;517.944

Questions involving interaction of laser radiation with material in the dispersed state (ice particle destruction) are considered.

As was shown in [1], action of intense radiation at a wavelength of 10.6 μm on lamellar ice crystals produces inhomogeneous temperature fields which lead to the appearance of elastic stress fields. For high inhomogeneity of the temperature field the temperature changes within the crystals can reach values such that tensile elastic stresses become greater than the failure stress for ice, equal to $2 \cdot 10^6$ N/m^2. In this case failure (cracking) of the crystal occurs with formation of smaller ice particles.

In the subcloud layer of crystalline or mixed clouds small ice particles of spherical or almost spherical form may exist. Like lamellar crystals, spherical ice particles can be destroyed by the action of intense radiation at λ = 10.6 μm due to inhomogeneous internal heat liberation, while not reaching the melting temperature. The present study will attempt to evaluate conditions and energy expenditures for thermal destruction of spherical ice particles under radiant action.

In the general case the ice particles have a hexagonal crystalline lattice with a weakly expressed anisotropy in both optical and elastic properties. However, real crystals formed in the atmosphere contain microimpurities, have large numbers of point defects and other structural faults, which under the conditions of the problem being considered allow us to consider the crystal as being isotropic. The heat liberation Q at a specified point within a homogeneous spherical particle with coordinates r, θ, ϕ is defined by the expression [2]

$$Q = \frac{4\pi n \varkappa}{m_m \lambda} IB, \tag{1}$$

where $B = (E, E_r^* + E_\theta E_\theta^* + E_\phi E_\phi^*) E_0^{-2}$. At λ = 10.6 μm for ice n = 1.097, κ = 0.134.

From the behavior of the curves of Fig. 1 it is evident that as in a water droplet [2], heat liberation within the ice particle volume is inhomogeneous, especially in particles with a radius $R \gg 10$ μm. In contrast to water droplets, here we find no large maxima in heat liberation near the dark surface of the particle. The major heat liberation occurs on the illuminated surface. This is explained by the fact that the real component of the index of refraction of ice is somewhat lower than that of water, while the imaginary component is significantly higher [3].

The problem of destruction of an ice crystal suspended in air under the action of thermoelastic stresses initiated by intense laser radiation reduces to simultaneous solution of the equilibrium [4] and thermal conductivity equations

$$\frac{3(1-\sigma)}{1+\sigma} \nabla \operatorname{div} \mathbf{u} - \frac{3(1-2\sigma)}{2(1+\sigma)} \operatorname{rot} \operatorname{rot} \mathbf{u} = \gamma \nabla T, \tag{2}$$

$$c\rho \frac{\partial T}{\partial t} = \lambda_1 \Delta T + Q(r, \theta, \varphi, n, \varkappa, \lambda, t, I) \tag{2a}$$

with appropriate boundary and initial conditions.

Physics Institute, Academy of Sciences of the Belorussian SSR, Minsk. Translated from Inzhenerno-Fizicheskii Zhurnal, Vol. 54, No. 1, pp. 103-108, January, 1988. Original article submitted October 16, 1986.

 0022-0841/88/5401-0080 $ 12.50 © 1988 Plenum Publishing Corporation